치의과학석사학위논문

Targeting XIAP in mucoepidermoid carcinoma of salivary gland: A novel therapeutic strategy of nitidine chloride

타액선 점액표피양암종에서 XIAP 단백질을 표적하는 Nitidine chloride의 항암효능 및 분자기전에 관한 연구

2019년 02월

서울대학교 대학원
치의과학과 구강병리학전공

권 혜 정

Targeting XIAP in mucoepidermoid carcinoma of salivary gland: A novel therapeutic strategy of nitidine chloride

타액선 점액표피양암종에서 XIAP 단백질을 표적하는 Nitidine chloride의 항암효능 및 분자기전에 관한 연구

지도교수 조성대

이 논문을 치의과학 석사학위논문으로 제출함

2018년 11월

서울대학교 대학원

치의과학과 구강병리학전공

권 혜 정

권혜정의 석사학위논문을 인준함

2018년 12월

위 원 장 홍 성 두 (인)

부 위 원 장 이 재 일 (인)

위 원 조 성 대 (인)

ABSTRACT

Targeting XIAP in mucoepidermoid carcinoma of salivary gland: A novel therapeutic strategy of nitidine chloride

Hye-Jeong Kwon

Oral Pathology major

The Graduate School

Seoul National University

(Directed by Professor Sung-Dae Cho, D.V.M., Ph.D.)

Background/Aims: Recently, nitidine chloride (NC) has been reported to exhibit a wide range of pharmacological properties for several diseases, including cancers. Based on the lack of information on the effects of NC in mucoepidermoid carcinoma (MEC), we report NC as a potential therapeutic agent because it suppresses XIAP in human MEC both *in vitro* and *in vivo*.

Methods: The antitumor effects of NC were evaluated by trypan blue exclusion assay, western blotting, live/dead assay, DAPI staining, human apoptosis antibody array, immunofluorescence staining, immunohistochemistry, small interfering RNA assay, transient transfection of XIAP overexpression vector, TUNEL assay, and histopathological examination of organs.

Results: NC inhibited cell viability and induced caspase-dependent apoptosis *in vitro*. The human apoptosis antibody array showed that XIAP was commonly suppressed by NC treatment. XIAP was overexpressed in oral tumor tissues, and high XIAP expression was correlated with poor prognosis in oral cancer patients. XIAP depletion significantly increased apoptosis and ectopic XIAP overexpression attenuated the apoptosis induced by NC treatment. NC suppressed tumor growth *in vivo* at a dosage of 5 mg/kg/day. TUNEL-positive cells increased, and the protein expression of XIAP was consistently downregulated in NC-treated tumor tissues. In addition, NC did not cause any histological changes to the liver or kidney.

Conclusion: Taken together, these findings provide new insight into the mechanism of action underlying the anti-cancer effects of NC, a

promising therapeutic agent for the treatment of human MEC of the salivary gland.

Keywords: Mucoepidermoid carcinoma of salivary gland, Nitidine chloride, XIAP, Apoptosis

Student Number: 2017-29534

TABLE OF CONTENTS

1. Introduction

Natural products isolated from vegetables, plants, microorganisms, and marine resources have historically been the main sources of therapeutic drugs. Natural products have the potential to treat chronic diseases, including cancer [1-4], and their use as anti-cancer agents has been continually developed because they offer high therapeutic efficiency and weak side-effects [5]. Indeed, many Food and Drug Administration-approved drugs derived from natural products are currently being used as broad-spectrum chemotherapeutic anti-cancer drugs in the clinic [6]. Nitidine chloride (NC) is a natural bioactive phytochemical alkaloid derived from the roots of *Zanthoxylum nitidum* that has been used as a traditional herbal medicine. Many previous studies have shown that NC has various beneficial biological properties, such as anti-inflammatory, anti-malarial, and anti-fungal effects [7-9]. The accumulated data suggest that the anti-cancer activity of NC involves inhibition of cell proliferation, cell cycle arrest, induction of apoptosis, and suppression of metastasis through multiple signal transduction pathways [10, 11]. Recently, our group found that NC induces apoptosis in oral squamous cell carcinoma (OSCC) both *in*

vitro and *in vivo* [12]. However, the potential therapeutic role of NC in mucoepidermoid carcinoma (MEC) of the salivary gland has not been studied previously.

The inhibitor of apoptosis proteins (IAPs) contain one to three baculovirus IAP repeat domains [13]. IAPs have the crucial ability to regulate cell survival and death by physically interacting with caspases [14, 15]. X-chromosome-linked IAP (XIAP), one of the IAP protein family, is an anti-apoptotic protein that contributes to cancer progression [16]. XIAP is over-expressed in a variety of cancers [17], and elevated XIAP expression is associated with poor prognosis and chemoresistance [18, 19]. In addition, it was reported that XIAP overexpression has a strong relationship with poor clinical outcomes among advanced head and neck squamous cell carcinoma (HNSCC) patients [20]. Thus, targeting XIAP using natural product-derived chemicals could be a promising chemotherapeutic approach for HNSCC, including MEC of the salivary gland. Therefore, our aim in this study was to investigate the significance of XIAP targeting using NC as a novel therapeutic strategy against human MEC of the salivary gland.

2. Materials and Methods

2.1 Cell culture and chemical treatment

YD-15 and MC-3 cell lines (human MEC) were obtained from Yonsei University (Seoul, Korea) and the Fourth Military Medical University (Xi'an, China), respectively. Cells were cultured in either RPMI1640 or DMEM/F-12 media supplemented with 10% fetal bovine serum and 100 U/ml penicillin and streptomycin at 37℃ in a 5% CO_2 incubator. All experiments were prepared after the cells reached 50~60% confluence. The cells were treated with NC (Figure 1A; Sigma-Aldrich Chemical Co., St. Louis, MO, USA) dissolved in dimethyl sulfoxide (DMSO). The final concentration of DMSO did not exceed 0.1%.

2.2 Reagents and antibodies

z-VAD was obtained from R&D Systems (Minneapolis, MN, USA), a Live/Dead & Viability/Cytotoxicity kit was provided by Life Technologies (Grand Island, NY, USA), and 4',6-diamidino-2-phenylindole (DAPI) was purchased from Sigma–Aldrich Chemical Co. (St Louis, MO, USA). Antibodies against cleaved caspase3, cleaved PARP, XIAP, Bcl-x, survivin, Bax, p-STAT3 (Y705), p-STAT3 (S727),

STAT3, and Mcl-1 were purchased from Cell Signaling Technology, Inc. (Charlottesville, VA, USA). Actin antibody was provided by Santa Cruz Biotechnology, Inc. (Santa Cruz, CA, USA).

2.3 Trypan blue exclusion assay

The effects of NC on cell viability were determined with trypan blue solution (Gibco, Paisley, UK). Cells were stained with 0.4% trypan blue solution, and viable cells were counted using a hemocytometer.

2.4 Western blotting

Whole cell lysates were extracted with RIPA lysis buffer (EMD Millipore, Billerica, CA, USA) containing phosphatase inhibitor and protease inhibitor cocktails, and the protein concentration of each sample was measured using a DC Protein Assay Kit (Bio-Rad Laboratories, Madison, WI, USA). After normalization, equal amounts of protein were separated by SDS-PAGE and transferred to Immuno-Blot PVDF membranes. The membranes were blocked with 5% skim milk at room temperature (RT) for 2 hr, incubated with the specific primary antibody overnight at 4℃, and probed with horseradish peroxidase (HRP)-conjugated secondary antibody for 2 hr at RT. The

bands were immune-reactivated with enhanced chemiluminescence (ECL) solution (Santa Cruz Biotechnology, Inc., Santa Cruz, CA, USA) and visualized on an ImageQuant LAS 500 (GE Healthcare Life Sciences, Piscataway, NJ, USA).

2.5 Live/dead assay

The cytotoxicity of NC was determined using a live/dead & viability/cytotoxicity assay. The polyanionic dye, calcein-AM is retained within live cells, producing intense green fluorescence through intracellular esterase activity. Ethidium homodimer-1 enters dead cells with damaged membranes and binds to nucleic acids, producing bright red fluorescence in dead cells. Briefly, cells were stained with 2 μM calcein-AM and 4 μM ethidium homodimer-1, and incubated for 30 min at RT. Cells were analyzed under a fluorescence microscope (Leica DMi8, Wetzlar, Germany) with the appropriate excitation and emission filters.

2.6 4',6-Diamidino-2-phenylindole staining

To identify nuclear morphological changes of apoptotic cells, the cells were stained with DAPI fluorescence dye. Briefly, cells were fixed

in 100% methanol at RT for 10 min, deposited on slides, and stained with DAPI solution (2 μg/ml). The morphological changes of apoptotic cells were observed under a fluorescence microscope.

2.7 Human apoptosis antibody array

Cells were treated with DMSO or 10 μM NC for 24 hr, and the relative expression of 35 apoptosis-related proteins was determined using a Human Apoptosis Antibody Array Kit (R&D Systems, Minneapolis, MN, USA). Briefly, nitrocellulose membranes were blocked with array buffer for 1 hr at RT. Protein lysates were then diluted, added, and incubated overnight. After washing with 1X wash buffer to remove unbound proteins, the membranes were exposed to a cocktail of biotinylated detection antibodies for 1 hr at RT and then incubated with streptavidin–HRP antibody for 30 min at RT. Each capture spot corresponding to the amount of apoptotic protein bound was detected with ECL western blotting luminol reagent. The intensity score of each duplicated spot was measured using ImageJ software. The locations of the control and capture antibodies are listed in Figure 11.

2.8 Immunofluorescence staining

YD-15 and MC-3 cells were seeded on 4-well culture plates and treated with DMSO or 10μM NC. After treatment for 24 hr, cells were fixed and permeabilized using Cytofix/Cytoperm solution for 1 hr at 4℃. Cells were then blocked with 1% BSA in PBS for 1 hr at RT and incubated overnight at 4℃ with XIAP antibody. Subsequently, the cells were exposed to the FITC-conjugated secondary antibody for 1 hr at RT and visualized using a fluorescence microscope equipped with the appropriate filters for DAPI and FITC dyes.

2.9 Clinical patient samples

Twenty-five oral cancer tissue samples and 10 normal oral mucosa (NOM) tissue samples were used for immunohistochemical testing. NOM tissues were acquired from adult patients without pathological lesions during third molar extraction, and oral cancer tissues were acquired from the archives of the Department of Pathology, Pusan National University, from January 2003 to December 2007. The cases selected, both paraffin-embedded tissue blocks and haematoxylin and eosin (H&E) slides, showed good preservation. This study was approved by the Institutional Review Board of Pusan National

University Yangsan Hospital (IRB approval number: PNUDH-2018-016).

2.10 Immunohistochemistry

For immunohistochemical (IHC) staining, 4 μm tissue sections were prepared and treated with an avidin–biotin complex (Vectastain Universal Elite ABC Kit; Vector Laboratories, Burlingame, CA, USA). IHC staining was performed using primary XIAP antibodies (1:50 dilution, Abcam, Cambridge, MA, USA). Antigen retrieval for the XIAP antibody was performed by boiling the slides in citrate buffer solution (pH 6.0; Invitrogen, CA, USA). The sections were visualized with freshly prepared 3,3'-diaminobenzidine tetrahydrochloride (Vector Laboratories) as the substrate, counterstained with Mayer's haematoxylin (Sigma-Aldrich, St Louis, MO, USA), dehydrated, and mounted. For each slide, five non-overlapping fields were randomly selected and photographed during examination using a Motic BA410 microscope with a Moticam Pro 205A (Motic Incoporated, Ltd., Causeway Bay, Hong Kong). A specialist in oral pathology assessed the histopathological conditions twice for each case. Positive staining was identified only in samples stained dark brown in the cytoplasm or

nucleus of oral epithelium (NOM) or tumor cells (oral cancer). The expression level of XIAP protein was evaluated using a semi-quantitative method. To evaluate the expression of XIAP, the level of immunoreactivity (LI) was defined as follows: The grade of XIAP expression was divided into five easily reproducible categories: (a) No detectable expression (point 0); (b) positive expression in 25% or fewer of cells (point 1); (c) positive expression in 26%–50% of cells (point 2); (d) positive expression in 51%–75% of cells (point 3), and (e) positive expression in more than 75% of cells (point 4). The intensity of XIAP expression was divided into four easily reproducible categories: (a) No detectable expression (point 0); (b) weak and diffuse staining (point 1); (c) moderate granular staining (point 2), and (d) strong and granular staining (point 3). LI was then calculated by multiplying XIAP grade by XIAP intensity. To divide the LI into LOW and HIGH expression groups, we calculated an average LI for all the oral cancer cases. The cases of oral cancer showing lower LI than the average were assigned to the LOW group, and the cases of oral cancer showing higher LI than the average were assigned to the HIGH group. The scoring was conducted blind to information about the oral cancer patients.

2.11 Small interfering RNA (siRNA) assay

A control nonspecific siRNA (siControl) and XIAP-targeted siRNA (siXIAP) were purchased from Santa Cruz Biotechnology. siRNA transfection was conducted using Lipofectamine 3000 transfection reagent (Life Technologies) following the manufacturer's instructions.

2.12 Construction of the XIAP overexpression vector and transient transfection

The open reading frame of human XIAP was amplified from cDNA using the specific primers of the gene (primer sequence: XIAP sense, 5'- GAA TTC ATG ACT TTT AAC AGT TTT GA -3', with an included *Eco*RI site, XIAP anti-sense, 5'- GAA TTC TTA AGA CAT AAA AAT TTT TTG C -3', with an included *Eco*RI site) and then cloned into pGEM T-easy vector (Promega, Madison, WI, USA). The XIAP was confirmed by sequence analysis. The gene was then cloned into the multi-cloning site of the pcDNA3.1 (+) vector (Invitrogen, San Diego, CA, USA). YD-15 and MC-3 cells were transfected with pcDNA3.1 and pcDNA3.1-XIAP vector constructs using Lipofectamine 3000 transfection reagent according to the manufacturer's instructions, respectively.

2.13 Nude mice tumor xenograft

Four-week-old female nude mice were purchased from NARA-Biotech (Pyeongtaek, Korea). All mice were handled according to the Institutional Animal Care and Use Committee (IACUC) guidelines approved by Kongju National University (IACUC approval number: KNU2018-4). MC-3 cells were inoculated into the flanks of the mice by subcutaneous (s.c.) injection. The mice were then randomly assigned to one of two treatment groups (n=6 for each group): the treatment group received 5 mg/kg/day of NC by intraperitoneal (i.p.) injection five times per week for 20 days, and the control group received an equal volume of vehicle (0.1% DMSO). Tumor volume and body weight were measured twice a week. After 20 days, tumor weight was measured. The tumor volumes were measured along the two diameter axes with calibers to allow calculation of tumor volume using the following formula: $V=\pi/6\{(D+d)/2\}^3$, where D and d are the larger and smaller diameters, respectively. Immunohistochemical staining was performed using primary XIAP antibody. Five non-overlapping fields were randomly selected and photographed during examination with a Nikon Eclipse E800 microscope.

2.14 Terminal deoxynucleotidyl transferase dUTP nick end labeling assay

Paraffin-embedded tumor tissues were analyzed using a terminal deoxynucleotidyl transferase dUTP nick end labeling (TUNEL) *in situ* apoptosis detection kit (DeadEnd Colorimetric TUNEL System, Promega, Madison, WI, USA) according to the manufacturer's instructions. Briefly, paraffin-embedded sections were deparaffinized and rehydrated. The sections were incubated with proteinase K for 15 min at RT, and the endogenous peroxidase was blocked with 0.3% hydrogen peroxide for 5 min. Digoxigenine-dUTP end-labeled DNA was detected using an anti-digoxigenin peroxidase antibody followed by peroxidase detection with 0.05% DAB containing 0.02% hydrogen peroxide. The sections were counterstained with methyl green, and the brown-colored apoptotic bodies in the tumor sections from control and NC-treated mice were counted using a Nikon Eclipse E800 microscope (Nikon Inc., Melville, NY, USA).

2.15 Histopathological examination of organs

Mouse organs (liver and kidney) were fixed in 10% neutral buffered formalin. Tissue sections were cut to a thickness of 4 μm and stained

with H&E. Histopathological changes were analyzed using a Nikon Eclipse E800 microscope.

2.16 Statistical analysis

For the *in vitro* study, statistical analysis was performed using GraphPad Prism software. A two-tailed Student's t-test was used to compare two experiments, and one-way ANOVA were applied for multiple comparisons with Tukey's post hoc test to determine the significance of differences between the control and treatment groups. Because the data were not normally distributed, we used Kruskal-Wallis testing to conduct a non-parametric analysis of differences between the NOM and oral cancer groups. Overall survival curves were created using the Kaplan–Meier method based on the expression of XIAP protein. Statistical significance was set at $p < 0.05$. Statistical analysis of the staining results was performed using SPSS version 23.0 (SPSS Inc. Chicago, IL, USA). For the *in vivo* study, statistical evaluation was performed using the Mann-Whitney U test in SPSS because our data were non-parametric. A p-value <0.05 was considered statistically significant.

3. Results

3.1 Nitidine chloride induces caspase-mediated apoptosis in human mucoepidermoid carcinoma cell lines

To explore the growth-inhibitory effect of NC MEC cell lines, we examined the cell viability of two cell lines (YD-15 and MC-3) after 24 hr of NC treatment. Treatment with NC clearly decreased cell viability in a concentration-dependent manner (Figure 1B). Fluorescence-based analysis of cell viability showed that NC increased the number of dead cells (red fluorescence, Figure 1C). We further investigated whether the growth-inhibitory effect was caused by NC-mediated apoptosis and found that NC caused morphological changes in nuclei, such as chromatin condensation and DNA fragmentation (Figure 2A). An additional analysis of the human MEC cell lines found that NC treatment effectively induced apoptosis, as evidenced by induction of cleaved caspase-3 and cleaved PARP (Figure 2B). To ascertain the involvement of caspase-3 in NC-induced apoptosis, both cell lines were treated with NC in the presence or absence of z-VAD, a pan-caspase inhibitor. The presence of z-VAD partially reduced NC-induced PARP cleavage (Figure 2C), indicating that caspase-3 activation serves as an

important mediator of NC-induced apoptosis. Overall, these findings provide evidence that NC has anti-proliferative and pro-apoptotic effects in human MEC cell lines.

3.2 Nitidine chloride reduces the expression level of XIAP protein in human MEC cell lines

To identify the apoptotic mediators that drive cell death in NC-treated MEC cell lines, we used a human apoptosis antibody array comprising 35 apoptosis-related proteins. The expression levels of XIAP, Bcl-x, and survivin (anti-apoptotic protein) in YD-15 cells were decreased by 0.86-fold, 0.77-fold, and 0.90-fold, respectively (Figure 3A). Those same three proteins were reduced in MC-3 cells by 0.66-fold, 0.75-fold, and 0.23-fold, respectively (Figure 3B). Conversely, the expression levels of Bax (pro-apoptotic protein) increased by 2.82-fold and 1.39-fold in YD-15 and MC-3 cells, respectively (Figures 3A and 3B). To verify the results from the human apoptosis antibody array, we used western blotting with antibodies able to detect those four proteins. In the western blotting results, only XIAP protein was reduced by NC treatment (Figure 4A). Immunofluorescence staining also showed a clear decrease in the expression of XIAP protein (Figure 4B). Thus,

inhibition of XIAP could be an important component of NC-mediated apoptosis in human MEC cell lines.

3.3 Upregulation of XIAP is in human oral cancer tissues correlates with poor prognosis in oral cancer patients

To investigate the clinical involvement of XIAP in oral cancer, the expression of XIAP in 10 normal oral mucosa (NOM) tissues and 25 oral cancer tissues was determined by IHC staining. XIAP was found to be more highly expressed in oral cancer tissues than in NOM tissues (Figure 5A). Consistently, IHC staining score of XIAP also showed that XIAP was significantly overexpressed in oral cancer tissues (Figure 5B). We further investigated the relationship between XIAP expression and the survival rate of patients. Kaplan-Meier analysis revealed a significantly higher survival rate for patients with low expression of XIAP protein (Figure 5C), suggesting that higher expression of XIAP correlates with poor prognosis in oral cancer patients. Collectively, our results show that XIAP could serve as a potential prognostic marker in human oral cancer.

3.4 XIAP silencing elicits apoptotic activity in human MEC cell lines

To determine the biological significance of elevated XIAP expression in human MEC cell lines, we performed loss-of-function experiments in human MEC cell lines using the siRNA-mediated silencing approach. XIAP silencing significantly suppressed cell viability (Figure 6A) and induced apoptotic cell death, as evidenced by induction of PARP cleavage and nuclear condensation and fragmentation (Figures 6B and 6C). These findings demonstrate that XIAP is required for growth of both YD-15 and MC-3 cell lines.

3.5 XIAP overexpression abrogates NC-induced apoptosis in human MEC cell lines

To further clarify the potential significance of XIAP in NC-induced apoptosis in human MEC cell lines, we performed gain-of function experiments using an XIAP overexpression system. Both cell lines were transfected with either a control or XIAP-overexpressing plasmid for 12 hr and then treated with 10 μM NC for 24 hr. Forced expression of XIAP partially attenuated NC-mediated growth inhibition and apoptosis in human MEC cell lines (Figures 7A and 7B), consistent

with the results from the fluorescence image analysis, which showed morphological changes in the nuclei (Figures 8A and 8B). These results suggest that XIAP plays a pivotal role in NC-induced apoptosis, and that the pro-apoptotic activity of NC is caused in part by suppression of XIAP expression.

3.6 NC has an anti-tumor effect without any liver or kidney toxicity in a mouse xenograft model

To extend our *in vitro* findings, nude mice were subcutaneously inoculated with MC-3 cells to investigate whether NC has an anti-tumor activity *in vivo*. The mice were received i.p. injections of vehicle control (0.1% DMSO) or NC (5 mg/kg/day) for 20 days. As shown in Figure 9A, NC administration significantly inhibited tumor volume compared with the vehicle control group (p=0.02). Consistently, tumor weight of the mice was reduced at the margin of statistical significance (p=0.07, Figure 9B). Based on stable body weight, we also found that NC administration did not show significant toxicity (Figure 9C). Further analysis revealed a near-significant increase in number of TUNEL-positive cells in the NC-treated group compared with the vehicle control group (p=0.06, Figure 9D). In addition, expression of

XIAP in the tumors of NC-treated mice was much lower than that in tumors of vehicle control-treated mice (p=0.008, Figure 10A), consistent with our *in vitro* observations. The histopathologic evaluation did not reveal any significant differences between the vehicle control- and NC-treated groups (Figure 10B). These results suggest that NC administration suppressed the tumor growth in our mouse xenograft model of human MEC without causing histopathological toxicity.

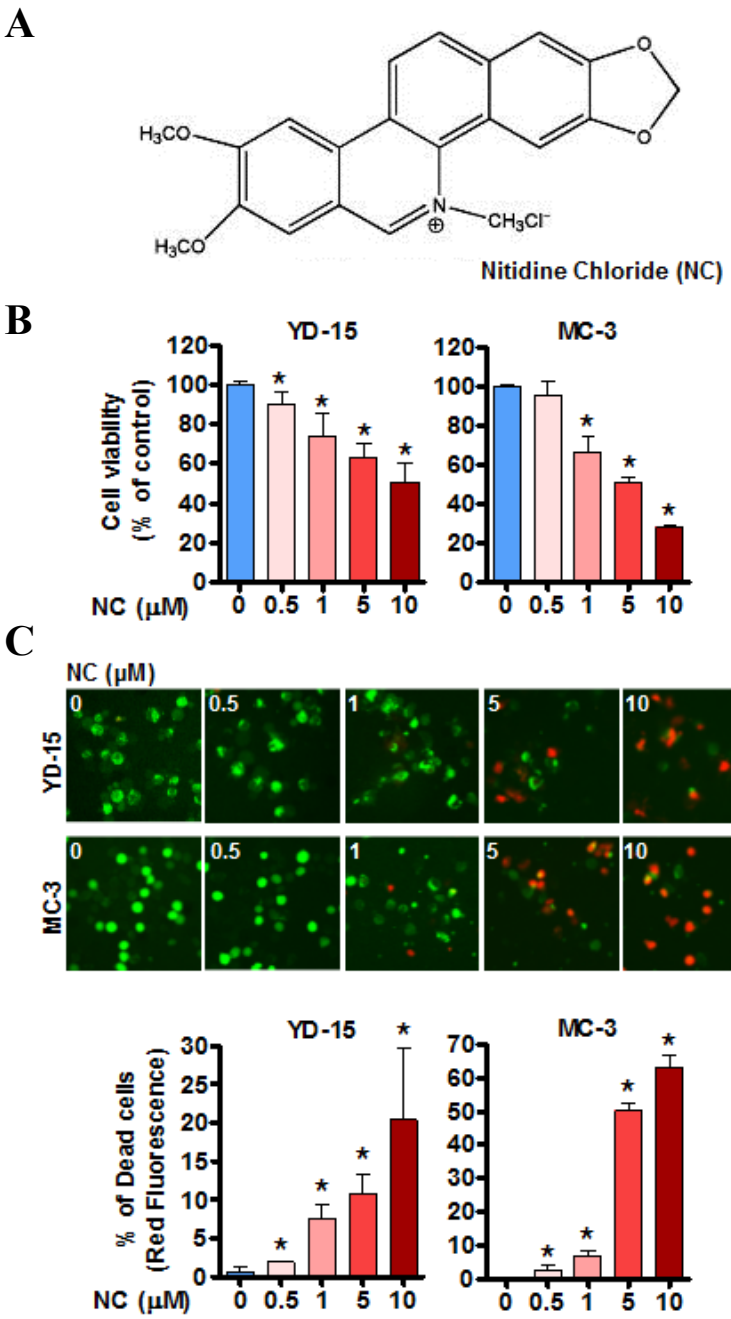

Figure 1. (A) The chemical structure of NC. **(B)** Cells were treated with DMSO or various concentrations of NC for 24 hr and cell viability

was determined using a trypan blue exclusion assay. The graphs represent the mean ± SD of three independent experiments and significance (p<0.05) compared with the DMSO treatment group is indicated (*). **(C)** Live (green fluorescence) and dead (red fluorescence) cells were observed by fluorescence microscopy. Representative images are shown (magnification, X200).

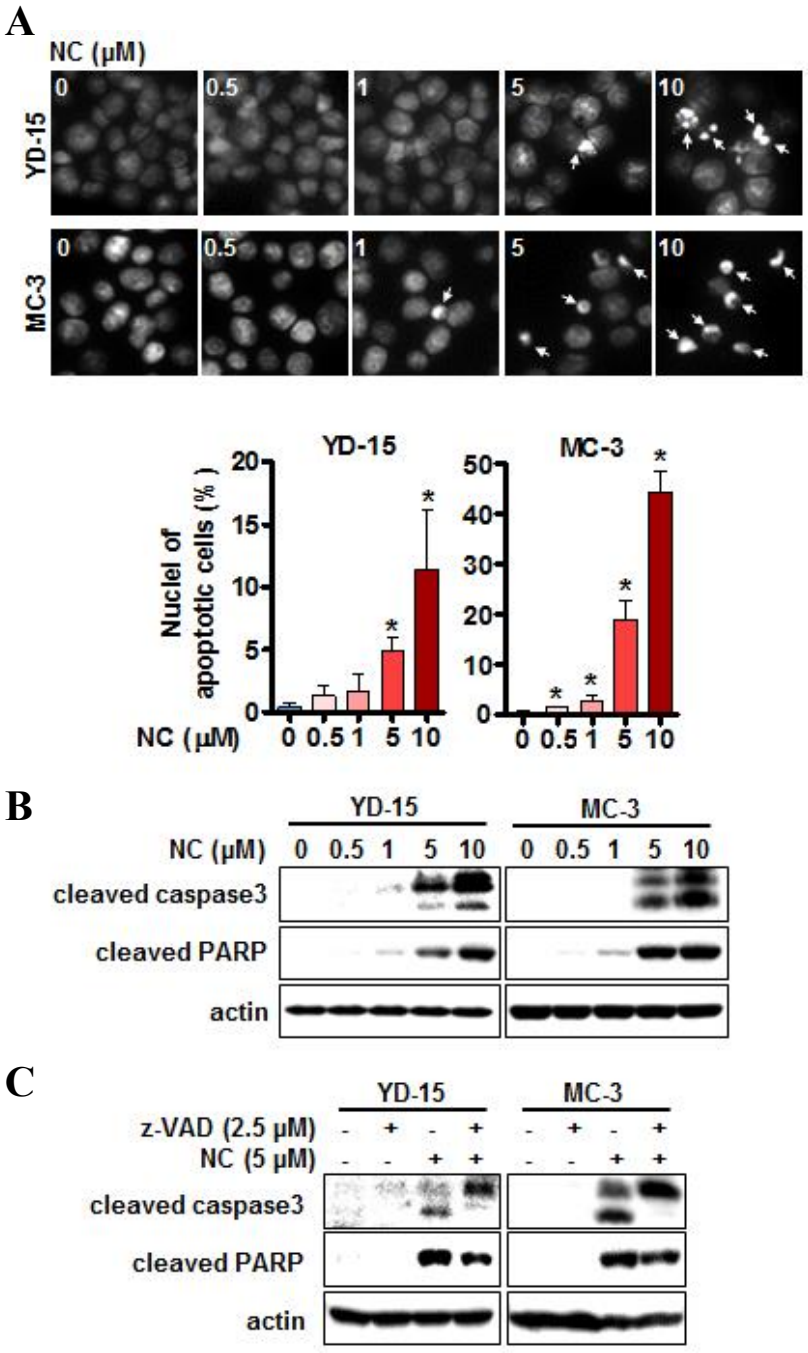

Figure 2. (A) Cells stained with DAPI solution were observed by fluorescence microscope. Representative images are shown

(magnification, X400). Graphs represent the mean ± SD of three independent experiments and significance (p<0.05) compared with the DMSO treatment group is indicated (*). **(B)** Protein levels of cleaved caspase 3 and PARP were determined by western blotting. **(C)** Cells were pretreated with z-VAD (a pan-caspase inhibitor) for 1 hr and then treated with DMSO or 5 μM NC for 24 hr. Protein lysates were analyzed by western blotting using antibodies against cleaved caspase3 and cleaved PARP. Actin was used as the loading control.

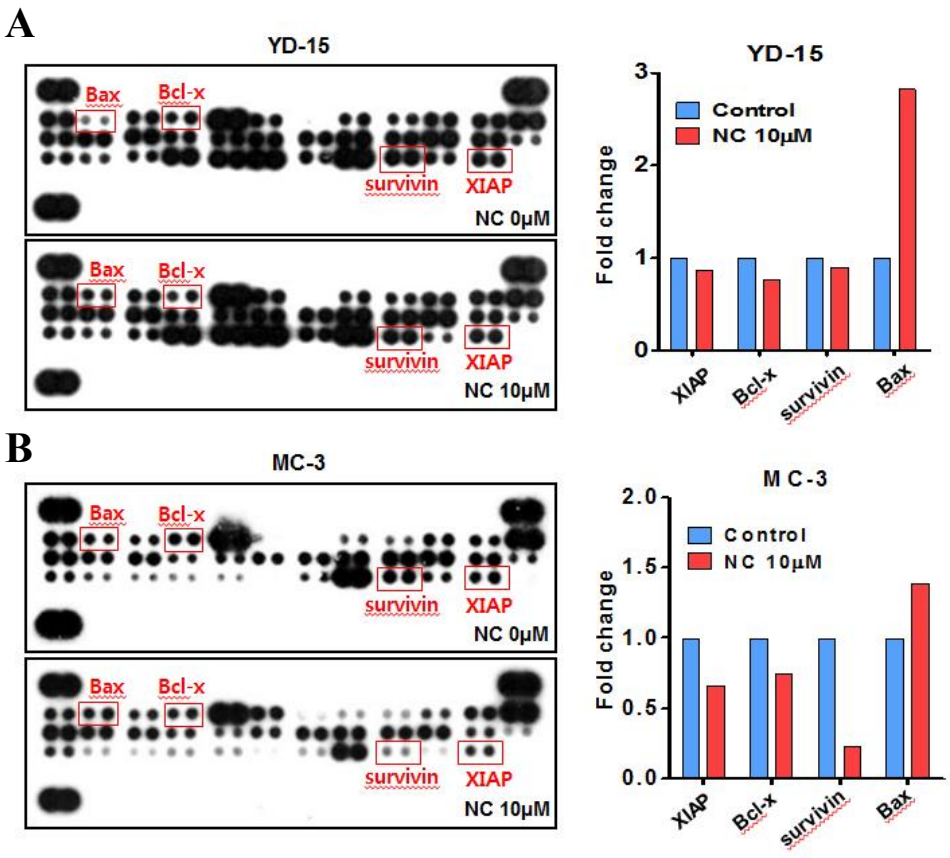

Figure 3. Results of human apoptosis antibody array in YD-15 **(A)** and MC-3 **(B)** cells. The graphs represent the relative spot intensities of each protein in two independent experiments.

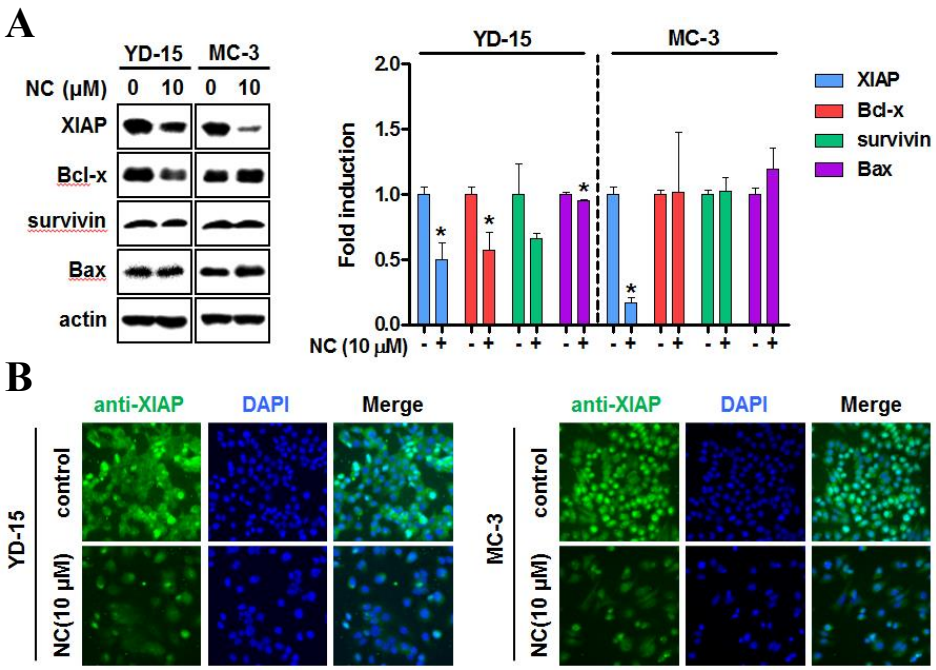

Figure 4. (A) Protein levels of XIAP, Bcl-x, survivin, and Bax were determined by western blotting. Actin was used as the loading control. The graphs represent the mean ± SD of three independent experiments, and significance (p<0.05) compared with the DMSO treatment group is indicated (*). **(B)** Immunofluorescence staining of XIAP in human MEC cell lines treated with NC. Representatives of the images for the staining of XIAP (green) and for nuclei counterstained with DAPI (blue) are shown. The merger panels combine the two images (magnification, X400).

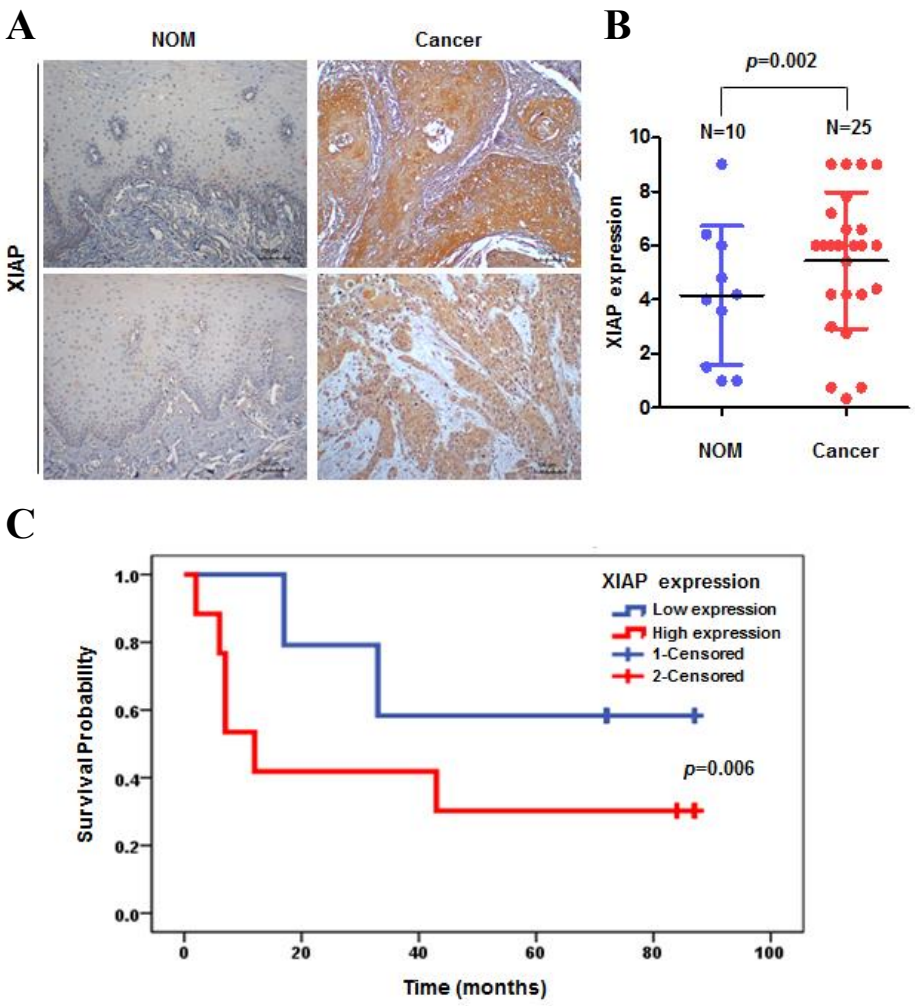

Figure 5. Immunohistochemical staining of XIAP and Kaplan-Meier survival plots for overall survival by XIAP status. **(A)** Normal oral mucosa (NOM) tissues and oral cancer tissues were prepared with XIAP antibody for IHC staining. Two representative images from each group are shown (magnification, X100). **(B)** IHC scores of XIAP in

NOM and oral cancer tissues. *p* values were calculated using the Kruskal-Wallis test. **(C)** Kaplan-Meier survival curves in oral cancer patients according to their IHC staining scores of low or high XIAP protein expression.

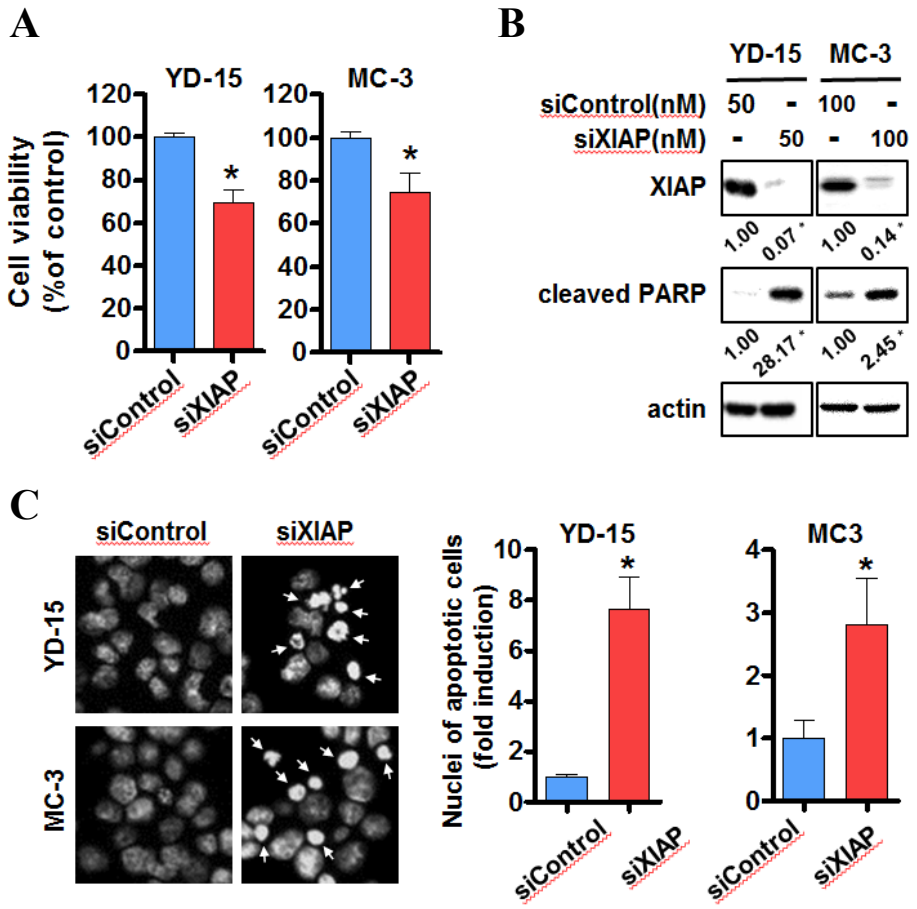

Figure 6. (A) Cells were transfected with siControl or siXIAP for different durations (48 hr for YD-15 and 72 hr for MC-3). Cell viability was examined using a trypan blue exclusion assay. **(B)** Protein levels of XIAP and cleaved PARP were analyzed by western blotting, and actin was used as the loading control. Data represent three independent experiments. **(C)** Nuclear staining using DAPI. Representative images are shown (magnification, X200). Graphs represent the mean ± SD of

three independent experiments. Significance ($p<0.05$) compared with the siControl-transfected group is indicated (*).

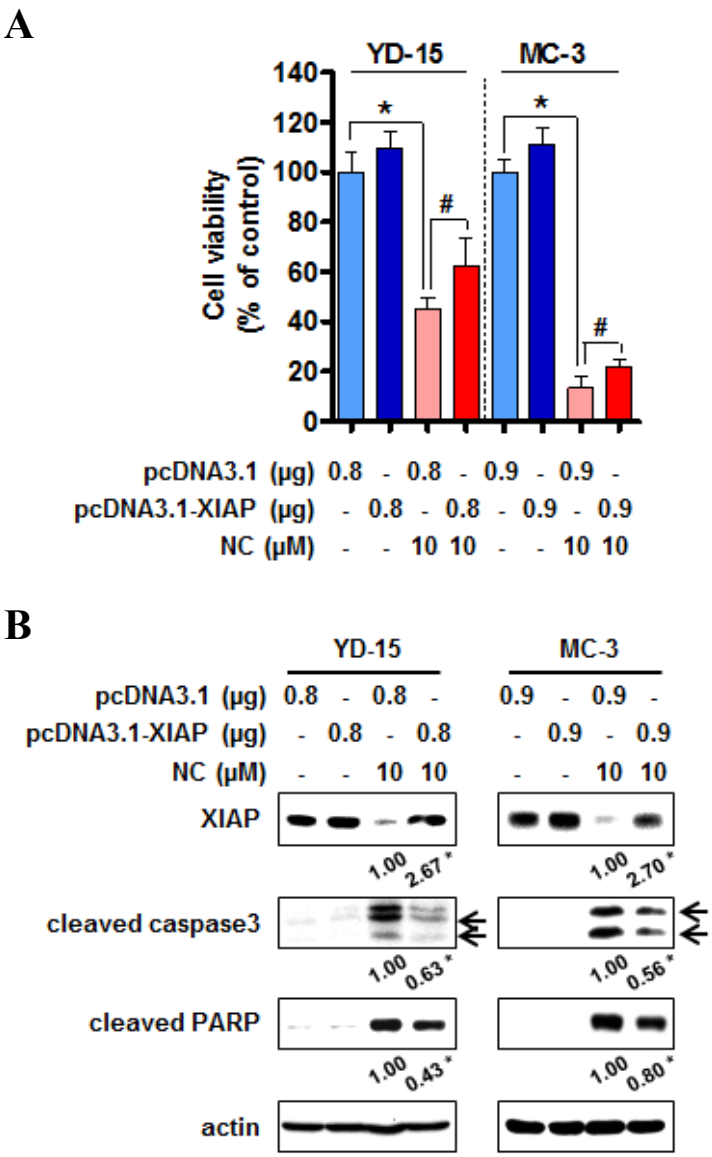

Figure 7. (A) Cells were transiently transfected with a pcDNA3.1 or pcDNA3.1-XIAP plasmid construct for 12 hr and then treated with 10 μM NC for 24 hr. Cell viability was determined using a trypan blue exclusion assay, and graphs represent the mean ± SD of three

independent experiments. *, $p<0.05$ compared with the DMSO-treated group after pcDNA3.1 transfection. #, $p<0.05$ compared with the NC-treated group after pcDNA3.1 transfection. **(B)** Whole cell lysates were prepared to detect the expression of XIAP, cleaved caspase3, and cleaved PARP using western blotting. Actin was used as the loading control. *, $p<0.05$ compared with the NC-treated group after pcDNA3.1 transfection.

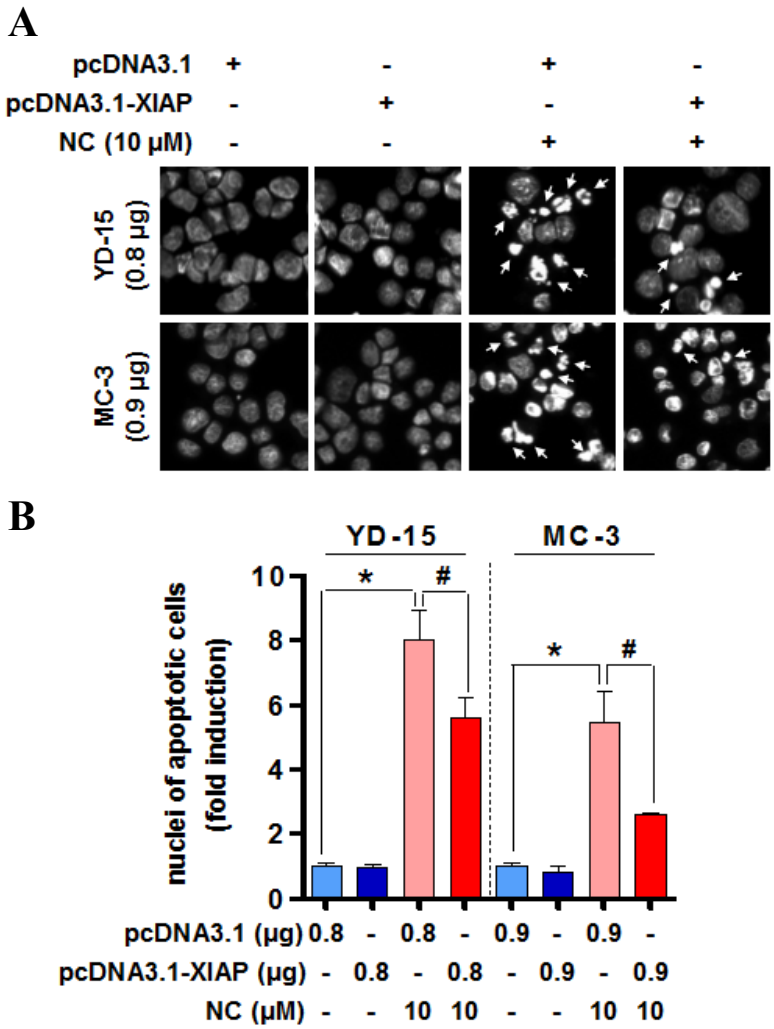

Figure 8. (A) Nuclear staining using DAPI. Representative images are shown (magnification, X400), and the arrows indicate morphological changes i.e. condensed or fragmented nuclei. **(B)** Graphs represent the mean ± SD of three independent experiments. *, $p<0.05$ compared with the DMSO-treated group after pcDNA3.1 transfection. #, $p<0.05$ compared with the NC-treated group after pcDNA3.1 transfection.

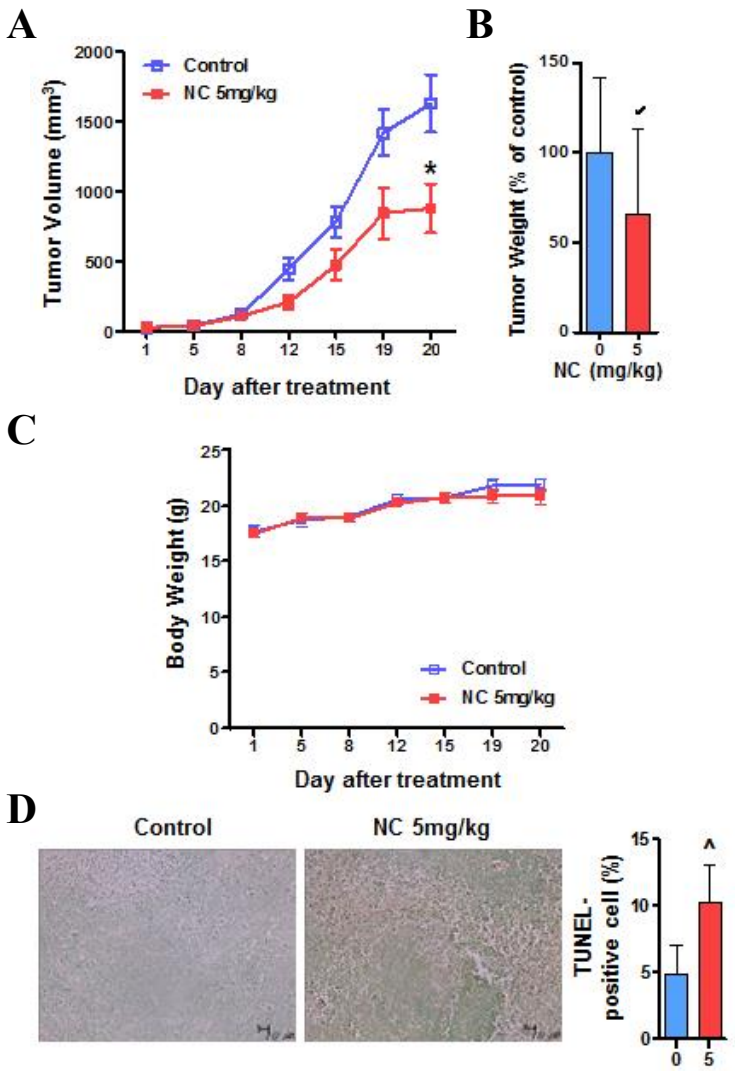

Figure 9. Nude mice implanted with MC-3 cells were administered with a vehicle control or 5 mg/kg/day of NC (i.p.) five times per week for 20 days. Tumor volume **(A)**, tumor weight **(B)**, and body weight **(C)** of the vehicle- and NC-treated groups were monitored as described in Materials and Methods. **(D)** Apoptotic effects of NC were determined by the TUNEL assay (magnification, X200).

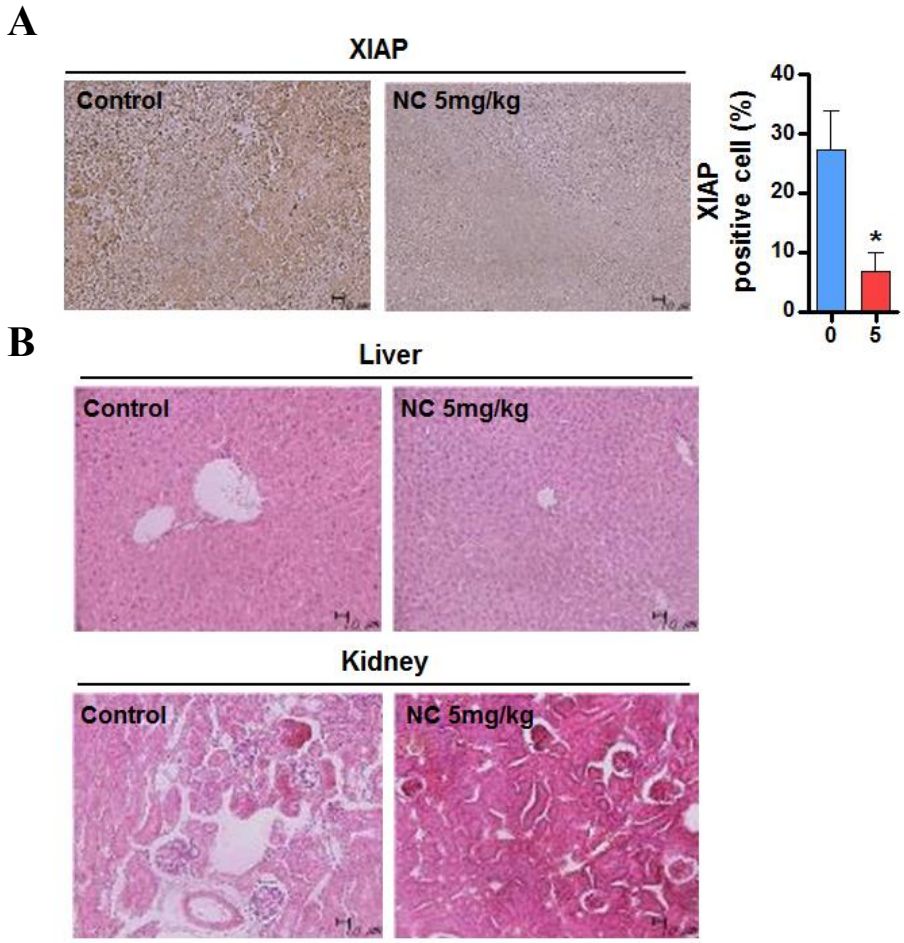

Figure 10. (A) IHC staining of XIAP in tumor tissues. Representative images are shown (magnification, X200). Graphs represent the mean ± SD, and significance (p<0.05) compared with the DMSO treatment group is indicated (*). **(B)** Histopathological images of liver and kidney sections stained by H&E (magnification, X200).

Human Apoptosis Array Coordinates

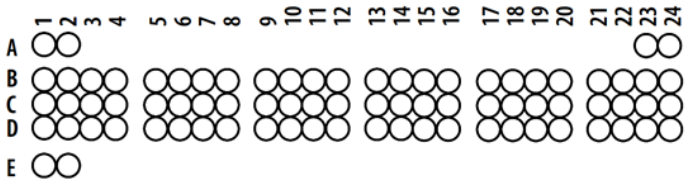

Coordinate	Target/Control	Coodinate	Target/Control
A1, A2	Reference Spots	C13, C14	HO-2/HMOX2
A23, A24	Reference Spots	C15, C16	HSP27
B1, B2	Bad	C17, C18	HSP60
B3, B4	Bax	C19, C20	HSP70
B5, B6	Bcl-2	C21, C22	HTRA2/Omi
B7, B8	Bcl-x	C23, C24	Livin
B9, B10	Pro-Caspase-3	D1, D2	PON2
B11, B12	Cleaved Caspase-3	D3, D4	p21/CIP1/CDKN1A
B13, B14	Catalase	D5, D6	p27/Kip1
B15, B16	cIAP-1	D7, D8	Phospho-p53 (S15)
B17, B18	cIAP-2	D9, D10	Phospho-p53 (S46)
B19, B20	Claspin	D11, D12	Phospho-p53 (S392)
B21, B22	Clusterin	D13, D14	Phospho-Rad17 (S635)
B23, B24	Cytochrome c	D15, D16	SMAC/Diablo
C1, C2	TRAIL R1/DR4	D17, D18	Survivin
C3, C4	TRAIL R2/DR5	D19, D20	TNF RI/TNFRSF1A
C5, C6	FADD	D21, D22	XIAP
C7, C8	Fas/TNFRSF6/CD95	D23, D24	PBS (Negative Control)
C9, C10	HIF-1α	E1, E2	Reference Spots
C11, C12	HO-1/HMOX1/HSP32		

Figure 11. Template presents the location of capture antibodies spotted onto a human apoptosis antibody array.

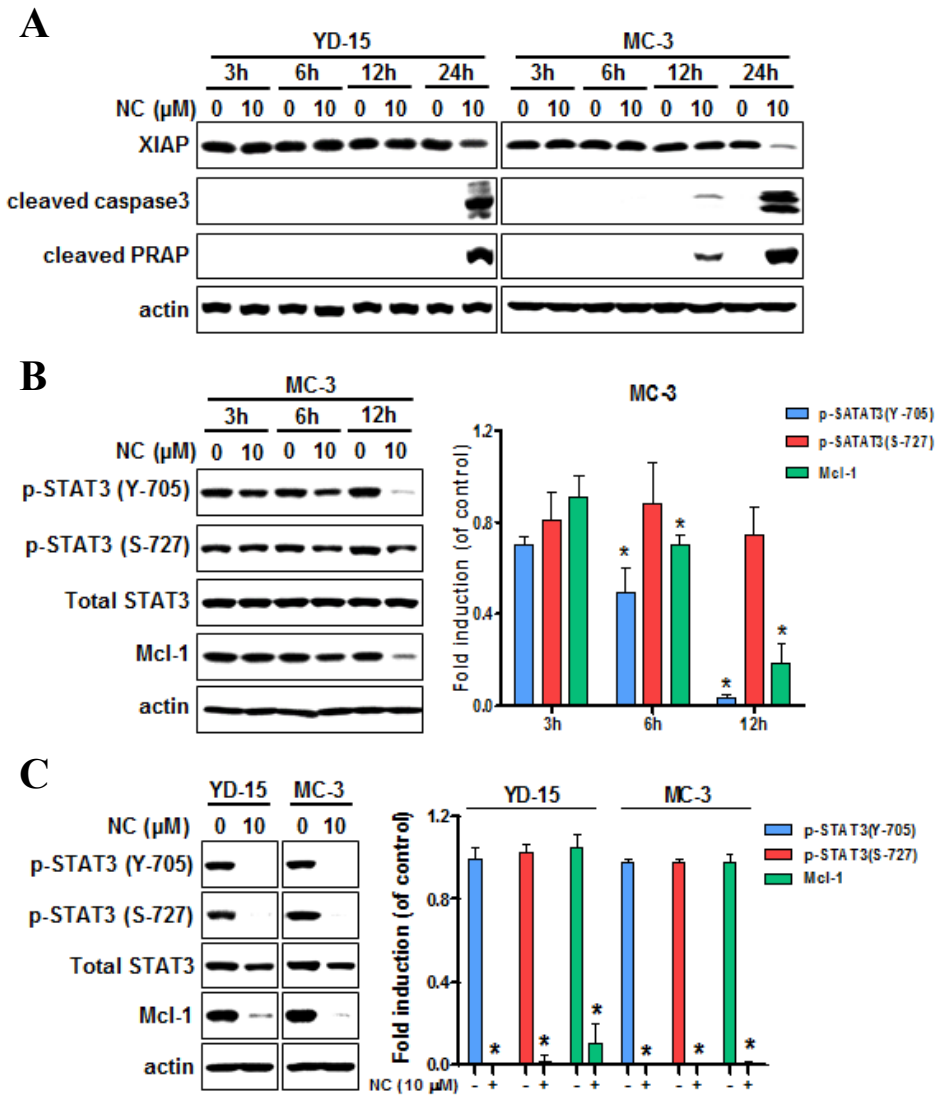

Figure 12. (A) Cells were treated with DMSO or 10 μM NC for various times. Protein levels of XIAP, cleaved caspase3, and cleaved PARP were determined by western blotting. **(B)** Protein levels of p-STAT3 (Y-705), p-STAT3 (S-727), total STAT3, and Mcl-1 were

determined by western blotting. **(C)** Cells were treated with DMSO or 10 μM NC for 24 hr. p-STAT3 (Y-705), p-STAT3 (S-727), total STAT3, and Mcl-1 proteins were detected by western blot analysis. Actin was used as the loading control. The graphs represent the mean ± SD of three independent experiments, and significance (p<0.05) compare with the DMSO treatment group at each time point is indicated (*).

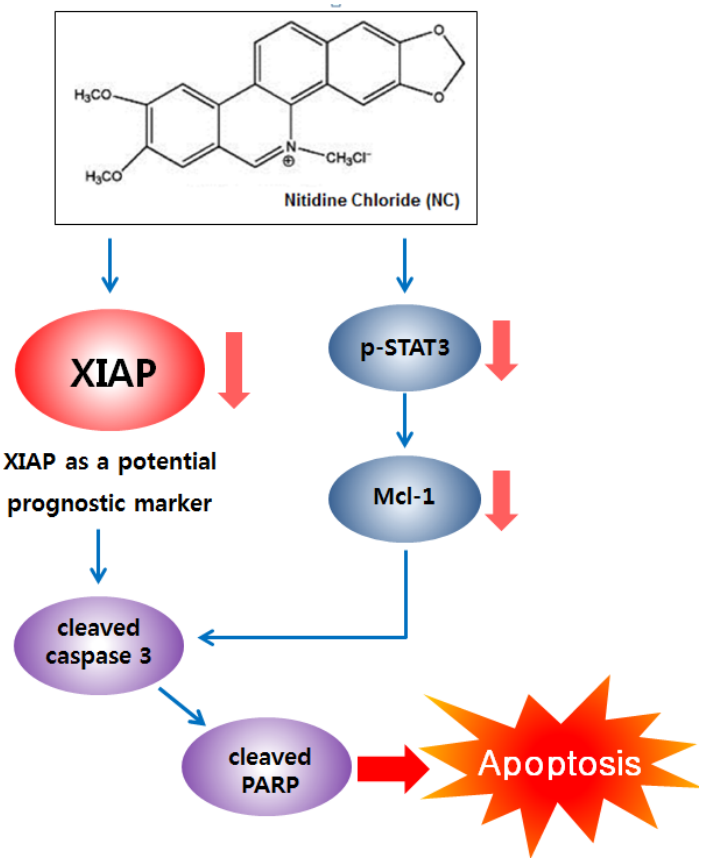

Figure 13. Schematic summary of the inhibitory effects of nitidine chloride on human mucoepidermoid carcinoma of salivary gland. Nitidine chloride suppresses the expression of XIAP protein as well as p-STAT3 and Mcl-1 signaling pathway in human MEC cell lines. In addition, XIAP may serve as a potential prognostic marker in human oral cancer. Finally, NC induces caspase-dependent apoptosis in human MEC of salivary gland.

5. Discussion

Mucoepidermoid carcinoma (MEC) is the most common histological subtype of salivary gland cancer which accounts for approximately 5% of head and neck malignancies [21]. Despite enormous development in diagnostic techniques and therapeutic options for many cancer patients, the standardization of effective systemic therapy for MEC patients is extremely limited due to their rarity. In the present study, we are the first to provide a promising chemotherapeutic strategy for the treatment of MEC by explaining the apoptotic effects and underlying mechanisms of NC in human MEC of the salivary gland *in vitro* and *in vivo*. First, NC treatment suppressed cell viability and induced apoptosis in human MEC cells *in vitro* and *in vivo*. Second, an aberrantly high expression of XIAP in oral cancer was associated with poor patient prognosis. Third, XIAP silencing markedly inhibited MEC cell viability by inducing apoptosis. Finally, ectopic expression of XIAP attenuated the effects of NC-mediated apoptosis in MEC cell lines.

In this study, we found that NC inhibited cell growth and induced caspase-dependent apoptosis in the YD-15 and MC-3 cell lines. Recently, several studies that investigated the apoptotic effects of NC in

ovarian, renal, gastric, and breast cancer found similar results [22-25]. Our findings are also in line with previous studies in our laboratory on the apoptotic effects of NC in oral cancer [12, 26]. Previous studies reported that intraperitoneal administration of NC at the effective dose (5 or 7 mg/kg/day) produced no obvious differences in body weight compared with a control-treated group [10, 25]. Consistent with those results, we found that NC treatment did not affect body weight or histopathological findings of the liver and kidney, implying that the anti-cancer effects of NC in human MEC of the salivary gland are not related to toxicity. Based on our results, we suggest that NC has potential as an apoptosis inducer to treat human MEC of the salivary gland without causing hepatic or renal toxicity.

The expression level of XIAP protein is associated with tumor recurrence and poor patient survival [13, 27]. It was reported that higher expression of XIAP is associated with decreased overall survival in all cases of OSCC [28] as well as malignant tumors of the salivary gland [29]. Consistent with those findings, our data demonstrated that XIAP is highly expressed in human oral cancer tissues and associated with poor prognosis. XIAP benefits cancer progression by blocking both the initiator and effector caspases that play important roles in

apoptosis [30]. Down-regulation of XIAP also contributes to sensitivity to chemotherapeutic drugs [31] and induction of apoptosis in other types of cancers [32, 33]. According to the results derived from human apoptosis antibody array, XIAP is commonly regulated by NC in human MEC of the salivary gland. XIAP depletion significantly inhibited cell viability and induced apoptosis, and overexpression of XIAP abrogated NC-induced apoptosis in human MEC cell lines. Lee's group [34] demonstrated that the XIAP inhibitor embelin can induce apoptosis in human oral cancer cell lines, in agreement with our present findings. Based on these results, we speculate that targeting XIAP using NC could be a promising therapeutic strategy for patients with MEC and other cancers.

We also investigated the time-dependent effects of NC on XIAP and induction of apoptosis in YD-15 and MC-3 cell lines. Unexpectedly, the expression levels of cleaved caspase-3 and cleaved PARP were detected in MC-3 cells earlier (12 hr) than the decrease in XIAP (24 hr), whereas NC simultaneously altered the expression patterns of the three proteins in YD-15 cells (Figure 12A). In addition, ectopic expression of XIAP partially attenuated the apoptotic effects of NC treatment. Although there are at least two explanations (pcDNA3.1 as a mild expression

promoter and transient transfection of XIAP), these results imply that another molecule could be involved in the NC-mediated apoptotic event. Thus, the question remains: what kinds of molecules other than XIAP protein contribute to NC-induced apoptosis at the early time point? Previously, several studies have reported that signal transducer and activator of transcription 3 (STAT3) might be positioned as an important chemotherapeutic target for NC treatment [25, 35]. Recently, our group also reported that NC functions as an apoptosis inducer by suppressing STAT3 and its downstream target myeloid cell leukemia-1 (Mcl-1) supporting other findings [12, 26]. Therefore, we further investigated whether STAT3 is indeed involved in anti-cancer effects of NC. STAT3 was significantly dephosphorylated (Y-705) in YD-15 cells at an early time point (6 hr), and its downstream target Mcl-1 was subsequently suppressed at a later time point in MC-3 cells (Figure 12B). In addition, NC decreased the expression levels of phospho-STAT3 and Mcl-1 at 24 hr (Figure 12C), suggesting that the STAT3/Mcl-1 signaling pathway is likely involved in NC-mediated apoptosis, like the XIAP protein.

There is no effective chemotherapy to treat MEC because of its rarity. Administration of single-agent therapy shows anti-tumor activity, but

overall response rates are not satisfactory [36, 37]. Recently, several studies reported that NC induced apoptosis and exhibits a synergistic cytotoxicity with doxorubicin in both ovarian and breast cancer cells [23, 38]. Although further studies are required to confirm its synergistic efficacy with other anticancer drugs for MEC, our data suggest the possibility to achieve the maximized anti-tumor effects with less toxicity by the combinational therapy of NC with conventional pro-apoptotic/chemotherapeutic agents in MEC.

6. Conclusion

In conclusion, our study provides novel compelling evidence that NC could serve as a potential therapeutic agent against human MEC via suppression of XIAP. These findings will help us discover a novel and innovative chemotherapeutic option for management of patients with human MEC of the salivary gland in the future.

7. Reference

1. da Rocha, M.D., et al., *The role of natural products in the discovery of new drug candidates for the treatment of neurodegenerative disorders II: Alzheimer's disease.* CNS Neurol Disord Drug Targets, 2011. **10**(2): p. 251-70.
2. Shukla, S.K., et al., *Cardiovascular friendly natural products: a promising approach in the management of CVD.* Nat Prod Res, 2010. **24**(9): p. 873-98.
3. Rios, J.L., F. Francini, and G.R. Schinella, *Natural Products for the Treatment of Type 2 Diabetes Mellitus.* Planta Med, 2015. **81**(12-13): p. 975-94.
4. Demain, A.L. and P. Vaishnav, *Natural products for cancer chemotherapy.* Microb Biotechnol, 2011. **4**(6): p. 687-99.
5. Gordaliza, M., *Natural products as leads to anticancer drugs.* Clin Transl Oncol, 2007. **9**(12): p. 767-76.
6. Li, F.S. and J.K. Weng, *Demystifying traditional herbal medicine with modern approach.* Nat Plants, 2017. **3**: p. 17109.
7. Wang, Z., et al., *Nitidine chloride inhibits LPS-induced inflammatory cytokines production via MAPK and NF-kappaB*

pathway in RAW 264.7 cells. J Ethnopharmacol, 2012. **144**(1): p. 145-50.

8. Bouquet, J., et al., *Biological activities of nitidine, a potential anti-malarial lead compound.* Malar J, 2012. **11**: p. 67.
9. Del Poeta, M., et al., *Comparison of in vitro activities of camptothecin and nitidine derivatives against fungal and cancer cells.* Antimicrob Agents Chemother, 1999. **43**(12): p. 2862-8.
10. Pan, X., et al., *Nitidine Chloride inhibits breast cancer cells migration and invasion by suppressing c-Src/FAK associated signaling pathway.* Cancer Lett, 2011. **313**(2): p. 181-91.
11. Li, P., et al., *Cell Cycle Arrest and Apoptosis Induction Activity of Nitidine Chloride on Acute Myeloid Leukemia Cells.* Med Chem, 2018. **14**(1): p. 60-66.
12. Kim, L.H., et al., *Nitidine chloride acts as an apoptosis inducer in human oral cancer cells and a nude mouse xenograft model via inhibition of STAT3.* Oncotarget, 2017. **8**(53): p. 91306-91315.
13. Obexer, P. and M.J. Ausserlechner, *X-linked inhibitor of apoptosis protein - a critical death resistance regulator and therapeutic target for personalized cancer therapy.* Front Oncol, 2014. **4**: p. 197.

14. Srinivasula, S.M. and J.D. Ashwell, *IAPs: what's in a name?* Mol Cell, 2008. **30**(2): p. 123-35.

15. Lopez, J. and P. Meier, *To fight or die - inhibitor of apoptosis proteins at the crossroad of innate immunity and death.* Curr Opin Cell Biol, 2010. **22**(6): p. 872-81.

16. Flanagan, L., et al., *High levels of X-linked Inhibitor-of-Apoptosis Protein (XIAP) are indicative of radio chemotherapy resistance in rectal cancer.* Radiat Oncol, 2015. **10**: p. 131.

17. Kashkar, H., *X-linked inhibitor of apoptosis: a chemoresistance factor or a hollow promise.* Clin Cancer Res, 2010. **16**(18): p. 4496-502.

18. Nakagawa, Y., et al., *IAP family protein expression correlates with poor outcome of multiple myeloma patients in association with chemotherapy-induced overexpression of multidrug resistance genes.* Am J Hematol, 2006. **81**(11): p. 824-31.

19. Mizutani, Y., et al., *Overexpression of XIAP expression in renal cell carcinoma predicts a worse prognosis.* Int J Oncol, 2007. **30**(4): p. 919-25.

20. Yang, X.H., et al., *XIAP is a predictor of cisplatin-based chemotherapy response and prognosis for patients with advanced*

head and neck cancer. PLoS One, 2012. **7**(3): p. e31601.

21. Rodriguez, C.P., et al., *Salivary Gland Malignancies.* Hematol Oncol Clin North Am, 2015. **29**(6): p. 1145-57.
22. Chen, S., L. Yang, and J. Feng, *Nitidine chloride inhibits proliferation and induces apoptosis in ovarian cancer cells by activating the Fas signalling pathway.* J Pharm Pharmacol, 2018. **70**(6): p. 778-786.
23. Sun, M., et al., *Nitidine chloride induces apoptosis, cell cycle arrest, and synergistic cytotoxicity with doxorubicin in breast cancer cells.* Tumour Biol, 2014. **35**(10): p. 10201-12.
24. Fang, Z., et al., *Nitidine chloride induces apoptosis and inhibits tumor cell proliferation via suppressing ERK signaling pathway in renal cancer.* Food Chem Toxicol, 2014. **66**: p. 210-6.
25. Chen, J., et al., *Inhibition of STAT3 signaling pathway by nitidine chloride suppressed the angiogenesis and growth of human gastric cancer.* Mol Cancer Ther, 2012. **11**(2): p. 277-87.
26. Yang, I.H., et al., *Nitidine chloride represses Mcl-1 protein via lysosomal degradation in oral squamous cell carcinoma.* J Oral Pathol Med, 2018.
27. Hussain, A.R., et al., *Role of X-Linked Inhibitor of Apoptosis as a*

Prognostic Marker and Therapeutic Target in Papillary Thyroid Carcinoma. J Clin Endocrinol Metab, 2015. **100**(7): p. E974-85.

28. Frohwitter, G., et al., *Site-specific gene expression patterns in oral cancer.* Head Face Med, 2017. **13**(1): p. 6.
29. Bagulkar, B.B., et al., *XIAP and Ki-67: A Correlation Between Antiapoptotic and Proliferative Marker Expression in Benign and Malignant Tumours of Salivary Gland: An Immunohistochemical Study.* J Clin Diagn Res, 2015. **9**(2): p. EC01-4.
30. Finlay, D., et al., *Inducing death in tumor cells: roles of the inhibitor of apoptosis proteins.* F1000Res, 2017. **6**: p. 587.
31. Schimmer, A.D., et al., *Small-molecule antagonists of apoptosis suppressor XIAP exhibit broad antitumor activity.* Cancer Cell, 2004. **5**(1): p. 25-35.
32. Gowda Saralamma, V.V., et al., *Inhibition of IAP's and activation of p53 leads to caspase-dependent apoptosis in gastric cancer cells treated with Scutellarein.* Oncotarget, 2018. **9**(5): p. 5993-6006.
33. Takeda, T., et al., *Bavachin induces the apoptosis of multiple myeloma cell lines by inhibiting the activation of nuclear factor kappa B and signal transducer and activator of transcription 3.*

Biomed Pharmacother, 2018. **100**: p. 486-494.

34. Lee, Y.J., et al., *XIAP inhibitor embelin induces autophagic and apoptotic cell death in human oral squamous cell carcinoma cells.* Environ Toxicol, 2017. **32**(11): p. 2371-2378.

35. Liao, J., et al., *Nitidine chloride inhibits hepatocellular carcinoma cell growth in vivo through the suppression of the JAK1/STAT3 signaling pathway.* Int J Mol Med, 2013. **32**(1): p. 79-84.

36. Grisanti, S., et al., *Cetuximab in the treatment of metastatic mucoepidermoid carcinoma of the salivary glands: a case report and review of literature.* J Med Case Rep, 2008. **2**: p. 320.

37. Posner, M.R., et al., *Chemotherapy of advanced salivary gland neoplasms.* Cancer, 1982. **50**(11): p. 2261-4.

38. Ding, F., et al., *Nitidine chloride inhibits proliferation, induces apoptosis via the Akt pathway and exhibits a synergistic effect with doxorubicin in ovarian cancer cells.* Mol Med Rep, 2016. **14**(3): p. 2853-9.

국 문 초 록

타액선 점액표피양암종에서 XIAP 단백질을 표적하는 Nitidine chloride의 항암효능 및 분자기전에 관한 연구

권 혜 정
서울대학교 대학원
치의과학과 구강병리학전공
지도교수 : 조 성 대

Nitidine chloride(NC)는 암을 포함한 다양한 질병에서 많은 약학적 특징을 보이는 것으로 알려져 있다. 하지만, 점액표피양암종에서 NC의 항암효능은 잘 알려져 있지 않다. 따라서 본 연구에서는 세포 및 동물실험에서 NC가 인간의 점액표피양암종에서 X-linked inhibitor of apoptosis protein(XIAP)를 억제하면서 항암제로서의 가능성을 보인다고 제시하고 있다. 본 연구에서 NC의 항종양 효능을 평가하기 위하여, trypan blue exclusion 분석, western blot 분석,

live/dead 분석, DAPI 염색, human apoptosis antibody 분석법, 면역 형광 염색법, 면역조직화학염색법, small interfering RNA 분석, XIAP 과발현 vector의 일시적인 transfection, TUNEL 분석, 장기의 병리조직학적 검사, 실험 방법들을 이용하였다. 연구결과, 세포실험에서 NC는 구강암세포의 생존능력을 억제시켰고 caspase 의존적 세포사멸을 유도하였다. Human apoptosis antibody 분석실험을 통해서, NC를 처리했을 때 두 종류의 구강암세포에서 XIAP의 단백질 발현이 공통적으로 억제되는 것을 확인했다. 구강암환자의 종양 조직에서 XIAP단백질은 과발현 되어있었고, XIAP의 높은 발현은 구강암 환자의 나쁜 예후와 관련이 있었다. 구강암세포에서 XIAP의 발현을 억제시켰을 때 세포사멸이 유도되었고, XIAP의 발현을 증가시켰을 때 NC에 의해 유도된 세포사멸이 부분적으로 억제되었다. 동물실험에서, 실험용 쥐에 NC를 5mg/kg/day로 복용시켰을 때 종양의 성장이 억제되었다. 또한 NC를 처리한 종양조직에서 TUNEL염색 양성세포가 증가하였고, 세포실험과 동일하게 XIAP의 단백질 발현이 억제되었다. 게다가, NC를 복용한 쥐에서 어떠한 조직학적 변화도 발견되지 않았다. 결론적으로, 본 연구는 타액선 점액표피양암종에서 NC의 항암효능과 분자기전을 증명하였고, 따라서 NC

가 구강암을 치료할 수 있는 잠재적인 항암물질로 발전가능성이 있다고 사료된다.

주요어 : 타액선 점액표피양암종, Nitidine chloride, XIAP, 세포사멸,

학 번 : 2017-29534